

## Isomeric decay of $^{208}\text{Ra}$

J. J. Ressler,<sup>1,2</sup> C. W. Beausang,<sup>1</sup> H. Ai,<sup>1</sup> H. Amro,<sup>1</sup> M. Babilon,<sup>1,3</sup> J. A. Caggiano,<sup>1,4</sup> R. F. Casten,<sup>1</sup> G. Gürdal,<sup>1,5</sup> A. Heinz,<sup>1</sup> R. O. Hughes,<sup>1,6</sup> E. A. McCutchan,<sup>1</sup> D. A. Meyer,<sup>1</sup> C. Plettner,<sup>1</sup> J. Qian,<sup>1</sup> M. J. S. Sciacchitano,<sup>1</sup> N. J. Thomas,<sup>1,6</sup> E. Williams,<sup>1</sup> and N. V. Zamfir<sup>1,7</sup>

<sup>1</sup>*A. W. Wright Nuclear Structure Laboratory, Yale University, New Haven, Connecticut 06520*

<sup>2</sup>*Department of Chemistry, Simon Fraser University, Burnaby, British Columbia, Canada V5A-1S6*

<sup>3</sup>*Institut für Kernphysik, Technische Universität Darmstadt, 64289 Darmstadt, Germany*

<sup>4</sup>*TRIUMF, 4004 Wesbrook Mall, Vancouver, British Columbia, Canada V6T-2A3*

<sup>5</sup>*Clark University, Worcester, Massachusetts 01610*

<sup>6</sup>*University of Surrey, Guilford, Surrey, GU2 7XH, United Kingdom*

<sup>7</sup>*National Institute for Physics and Nuclear Engineering, Bucharest-Magurele, Romania*

(Received 20 August 2004; published 10 January 2005)

Low-energy excited states of  $^{208}\text{Ra}$  were investigated using the  $^{182}\text{W}(^{30}\text{Si}, 4n)$  reaction at the Wright Nuclear Structure Laboratory of Yale University. Fusion evaporation recoils were selected using the gas-filled spectrometer SASSYER. Delayed  $\gamma$  rays, following isomeric decays, were detected at the focal plane of SASSYER with a small array of three clover Ge detectors. Transitions following a proposed  $J^\pi = 8^+$  isomer were observed, and the half-life was measured.

DOI: 10.1103/PhysRevC.71.014302

PACS number(s): 23.20.Lv, 21.10.Tg, 25.70.Gh, 27.80.+w

### I. INTRODUCTION

The Po and Rn nuclei have recently become a popular arena to study the onset of collectivity as neutron numbers decrease from  $N = 126$ . Coexisting semispherical and vibrational structures have been observed, as well as deformed states at low neutron numbers (see Refs. [1,2] and references therein).

Systematic studies of the Po and Rn isotopes show the presence of secondary low spin states appearing near  $N = 120$ , and decreasing in energy as the neutron number declines. This secondary structure is thought to be more deformed than the dominant semispherical states closer to  $N = 126$ . Similar systematic studies have not yet been performed for the Ra isotopes; detailed structural information is only known for the  $^{214}\text{Ra}_{126}$  [3],  $^{212}\text{Ra}_{124}$  [4], and  $^{210}\text{Ra}_{122}$  [5] nuclei. For the Th isotopes, no structural information below  $N = 126$  is available [6]. Studies of these heavy proton-rich nuclei provide a challenge for experimentalists as fission becomes the dominant deexcitation channel and fusion evaporation cross sections decrease.

Studies in this region also provide a good test of seniority as both proton and neutron numbers move away from magicity. The  $N = 126$ , 124, and 122 isotones of Po, Rn, and Ra are excellent examples of the simple seniority scheme [7] for protons filling the  $1h_{9/2}$  orbital. Data for  $^{208}\text{Ra}_{120}$  provided here show the possible breakdown of this concept as more valence neutron (holes) are added.

### II. EXPERIMENT

The experiment was performed at the Wright Nuclear Structure Laboratory. Light Ra and Fr isotopes were produced following bombardment of an isotopically pure (94.32%) target of  $^{182}\text{WO}_3$  ( $460 \mu\text{g}/\text{cm}^2$ ) with 151 MeV  $^{30}\text{Si}$  ions provided by the ESTU Tandem accelerator. Other isotopes

present in the target were  $^{183}\text{W}$  (2.54%),  $^{184}\text{W}$  (2.32%),  $^{186}\text{W}$  (0.82%), and  $^{180}\text{W}$  (<0.05%) [8].

The Small Angle Separator System at Yale for Evaporation Residues (SASSYER, [9]) was used to select fusion evaporation recoil events. The spectrometer was filled with  $\sim 1$  Torr He gas and tuned to select  $A \sim 208$  recoils with a  $B\rho \approx 1.8$  T m. Fission products and unreacted beam particles will typically have a much lower rigidity and were therefore bent into a beam dump located at the first dipole. A thin ( $50 \mu\text{g}/\text{cm}^2$ ) carbon foil approximately 1 m upstream from the target was used to contain the He gas. The 151-MeV  $^{30}\text{Si}$  ions lost  $\sim 0.5$  MeV in the carbon window before reaching the target.

Following separation, recoils were implanted into a 30-element Si solar cell array. Each solar cell covered an area of  $1 \text{ cm}^2$ ; the entire array was 10 cm wide by 3 cm high. The solar cell array provided position, energy, and relative time information for the detection of the fusion recoils.

Three clover detectors, of 150% relative efficiency each, were placed around the thin aluminum chamber housing the solar cell array. Two clovers were placed on opposite sides, facing the sides of the array, and the third was placed directly behind the array. The clover detectors were used to observe delayed gamma decays depopulating isomeric states within  $3 \mu\text{s}$  following a recoil implantation.

An event in any one of the solar cells prompted readout of all detectors used in the setup. With an average beam current of  $I_b \approx 11 \text{ nA}$ ,  $1.77 \times 10^6$  recoils,  $2.80 \times 10^4$  recoil- $\gamma_{\text{delayed}}$  and  $0.25 \times 10^4$  recoil- $\gamma_{\text{delayed}}^n$  ( $n \geq 2$ ) coincidence events were collected in 94 hours.

### III. RESULTS

Delayed transitions occurring within  $3 \mu\text{s}$  following a recoil implantation are shown in Fig. 1(a). Numerous peaks are observed and may be assigned to Ra and Fr isotopes using

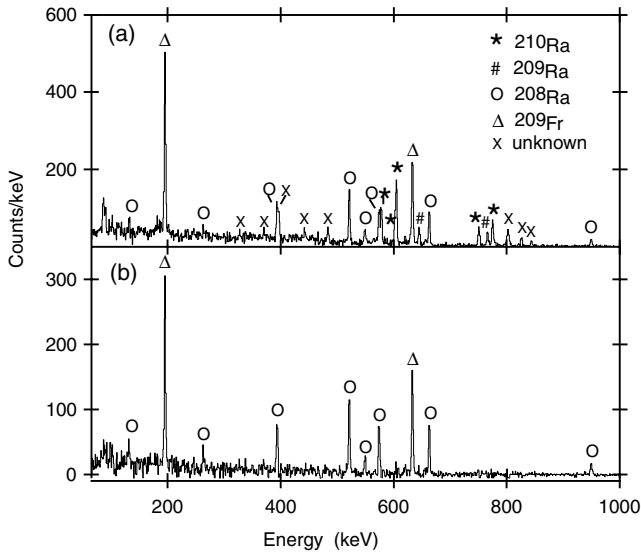


FIG. 1. (a) Delayed  $\gamma$  transitions observed within  $3 \mu\text{s}$  following a recoil implantation in the solar cell array. Most transitions may be assigned to  $^{210,209,208}\text{Ra}$  and  $^{209}\text{Fr}$  isotopes. (b) Time-subtracted isomer transitions; the spectrum of  $\gamma$ -ray energies detected within  $1\text{--}2.5 \mu\text{s}$  were subtracted from the spectrum collected within  $0\text{--}800$  ns after a recoil. Only short-lived species are observed.

weak coincidences with the corresponding x rays. Transitions belonging to  $^{210}\text{Ra}$  and  $^{209}\text{Ra}$  are largely due to the target contamination of heavier W isotopes. The  $^{210}\text{Ra}$  and  $^{209}\text{Ra}$  transitions have been studied previously [5], while  $^{208}\text{Ra}$  and  $^{209}\text{Fr}$  are new.

Earlier work by Cocks *et al.* [10] first identified the isomer in  $^{208}\text{Ra}$  and suggested a 270-ns half-life. This is significantly shorter than the  $2.1(1)\text{-}\mu\text{s}$  half-life of the  $8^+$  isomer of  $^{210}\text{Ra}$  and the suggested half-lives (one of  $t_{1/2} \sim \mu\text{s}$  and one of  $t_{1/2} \sim 10$ 's of  $\mu\text{s}$ ) for  $^{209}\text{Ra}$  [5]. To select only short-lived species in the isomer spectrum, transitions occurring within  $1$  to  $2.5 \mu\text{s}$  were subtracted from transitions within  $0$  to  $800$  ns following a recoil event. Longer-lived decays subtract to zero, while transitions from shorter half-lives appear as peaks. The subtracted spectrum, displayed in Fig. 1(b), shows only  $^{208}\text{Ra}$  and  $^{209}\text{Fr}$  peaks.

The time difference between recoil and delayed gamma events was used to measure decay half-lives of the transitions. For  $^{208}\text{Ra}$ , a weighted least-squares fit to the time spectra of the 520-, 548-, 661-, and 948-keV transitions was used to determine a half-life of 250(30) ns. The 130-, 262-, 392-, and 573-keV  $\gamma$  rays assigned to  $^{208}\text{Ra}$  were not used due to their low intensity or possible contamination from other nuclei produced in the reaction. The measured half-life is in excellent agreement with the 270-ns half-life proposed by Ref. [10]. For  $^{209}\text{Fr}$ , a half-life of 450(50) ns was measured using the 194- and 632-keV transitions. Decay curves of both  $^{208}\text{Ra}$  and  $^{209}\text{Fr}$  are shown in Fig. 2. A superior investigation of  $^{209}\text{Fr}$  has been performed by Meyer *et al.* and will be discussed in a subsequent paper [11].

Numerous weaker transitions were also observed in the isomer detectors. Table I lists the observed  $\gamma$ -ray energies and associated intensities for the delayed transitions within

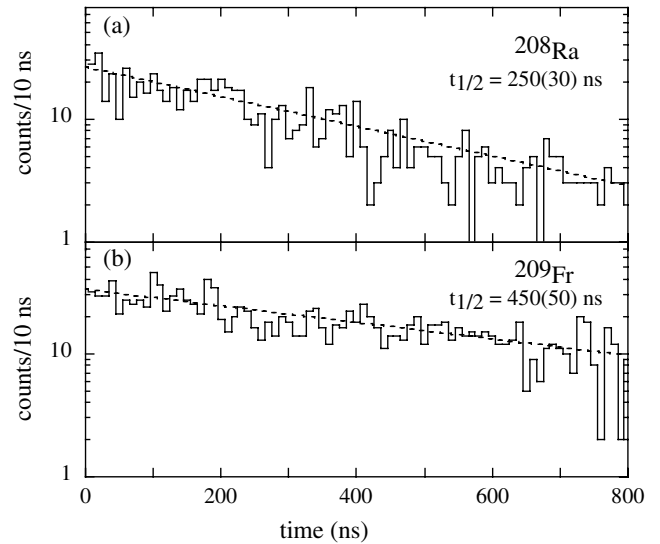


FIG. 2. (a) Decay curve for the deexcitation of the proposed  $8^+$  isomer in  $^{208}\text{Ra}$ . The summed intensity for the 520-, 548-, 661-, and 948-keV transitions is shown as a function of time following a recoil implantation in the solar cell array. Using a weighted least-squares fit, a half-life of 250(30)-ns is suggested. The dashed line shows a 250-ns decay half-life. (b) Decay curve for an isomer in  $^{209}\text{Fr}$ . A weighted least-squares fit to the 194- and 632-keV data results in a 450(50)-ns half-life. The dashed line represents a 450-ns decay.

$3 \mu\text{s}$  following a recoil implantation. Intensities shown have been approximately corrected for relative efficiency. This was accomplished by placing  $^{152}\text{Eu}$  and  $^{133}\text{Ba}$  sources near the center of the solar cell array and making the gross assumption that the radiation emitted from the  $30\text{-cm}^2$  solar cell array is similar to a point source.

Coincidences between the focal plane Ge detectors were very weak for the strongest transitions, and unavailable for the weaker. For the proposed  $^{208}\text{Ra}$   $\gamma$  rays, weak coincidences were used to build the level scheme below the isomer shown in Fig. 3.

In  $^{208}\text{Ra}$ , five excited levels are observed below the 250-ns isomer. The decay pattern is similar to the isotope  $^{206}\text{Rn}$ , where two  $6^+$  and two  $4^+$  states are observed below an  $8^+$  isomer [12]. If the spin and parity of the  $^{208}\text{Ra}$  isomer is assumed to be  $J^\pi = 8^+$ , similar to other nuclei in this region, the two states fed by the isomer may have  $J^\pi = 6^+$ . These states then decay into two separate ( $4^+$ ) states, which both feed the first excited  $2^+$  state. All spins and parities proposed here are not proven, but they agree with the observed intensity balances and systematic expectations from neighboring nuclei. Intensities corrected for internal conversion contributions assuming this decay scheme are shown in Table I.

The ordering of the  $6_2^+ \rightarrow 4_2^+$  and  $4_2^+ \rightarrow 2^+$  transitions may be reversed. The same is true for the  $6_1^+ \rightarrow 4_1^+$  and  $4_1^+ \rightarrow 2^+$  transitions. The ordering of these  $\gamma$  rays within  $^{208}\text{Ra}$  was assumed from comparisons to neighboring nuclei.

#### IV. DISCUSSION

For the Po, Rn, and Ra isotopes near  $N = 126$ , the  $1h_{9/2}$ ,  $2f_{7/2}$ , and  $1i_{13/2}$  proton orbitals dominate the low-energy

TABLE I.  $\gamma$ -ray energies and relative intensities observed in the isomer detectors. Also shown are multiplicities and intensities including internal conversion contributions [13] for transitions assigned to  $^{208}\text{Ra}$ . The isomer detectors are sensitive to half-lives within the microsecond range.

	$E_\gamma$ (keV)	$I_\gamma^a$	Multipolarity and $I_{\text{tot}}^b$
$^{208}\text{Ra}$ :			
	130.2(5)	13(3)	E2; 55(11)
	262.0(5)	12(2)	M1; 23(5)
	392.2(5)	43(7)	E2; 45(8)
	519.9(5)	100	E2; 100
	548.1(5)	31(5)	E2; 31(5)
	573.2(5)	70(10)	E2; 70(10)
	661.5(5)	69(9)	E2; 68(9)
	948.2(5)	27(4)	E2; 26(4)
$^{209}\text{Fr}$ :			
	193.8(5)	172(15)	
	631.5(5)	211(20)	
$^{210}\text{Ra}$ :			
	95(1)	5.5(3.0)	E2; 69(34)
	577.1(5)	83(10)	E2; 82(10)
	600.5(6)	46(6)	E2; 45(6)
	603.4(5)	151(18)	E2; 149(18)
	749.4(5)	52(7)	E2; 51(7)
	773.9(5)	82(10)	E2; 81(9)
$^{209}\text{Ra}$ :			
	643.6(5)	39(6)	E2; 38(6)
	764.9(5)	39(6)	E2; 38(6)
Other:			
	326.2(5)	7(3)	
	369.2(5)	12(4)	
	395.1(2)	46(8)	
	441.2(7)	19(5)	
	482.5(5)	28(5)	
	618.7(6)	11(3)	
	655(1)	11(1)	
	801.1(5)	63(8)	
	820(1)	5(2)	
	824.9(5)	24(4)	
	842.7(7)	12(3)	

<sup>a</sup>Relative to the 520-keV transition.

<sup>b</sup>Intensity with internal conversion corrections [13], relative to the 520-keV transition.

excitations. Neutrons in the  $2f_{5/2}$  and  $3p_{3/2}$  orbitals may also play a role [5,14].

The strongly populated, low-energy  $2^+$ ,  $4^+$ ,  $6^+$ , and  $8^+$  states in this region are attributed to a pair of protons in the  $1h_{9/2}$  orbital. The energy difference between the  $8^+$  and  $6^+$  levels is small, retarding the decay from the  $8^+ \rightarrow 6^+$  and yielding  $8^+$  isomeric states. A recent study has shown how the trends for the  $8^+ \rightarrow 6^+$  isomeric transitions can be described with a simple seniority scheme [7]. For seniority-conserving transitions (such as the  $8^+ \rightarrow 6^+$ ), a bowl-shaped trend is predicted and observed for the  $B(E2)$  values as a function of protons filling the  $1h_{9/2}$  orbital; see Fig. 4. These seniority-

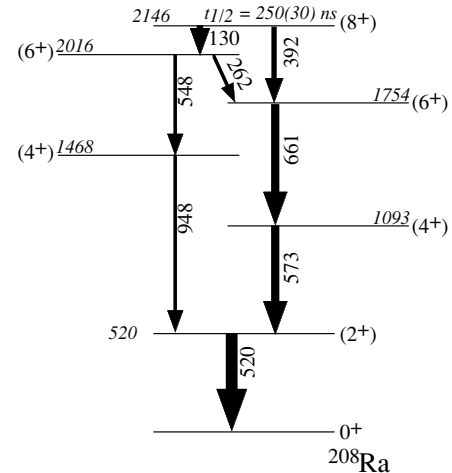


FIG. 3. Proposed level scheme for  $^{208}\text{Ra}$ . The relative intensity is denoted by the arrow width.

conserving transitions have been identified in the Po, Rn, and Ra isotopes with  $122 \leq N \leq 126$ .

However, as proton and neutron numbers move away from magicity, the seniority quantum number becomes less useful. Quasiparticle excitations may become energetically favorable; in the Po-Rn-Ra region,  $\pi 1h_{9/2}\pi 2f_{7/2}$  and  $\pi 2f_{7/2}^2$  configurations may compete with  $\pi 1h_{9/2}^2$ . In addition, collective states from vibrations or rotations may also alter the low-energy spectrum.

For the  $N = 120$  isotones, seniority is a questionable concept. The  $B(E2; 8^+ \rightarrow 6^+)$  values for  $^{204}\text{Po}$  and  $^{206}\text{Rn}$  are 3.5(2) [12] and 2.42(20) W.u. [15], respectively. Although the  $B(E2)$  value decreases with  $Z$ , the measured  $B(E2)$  value for

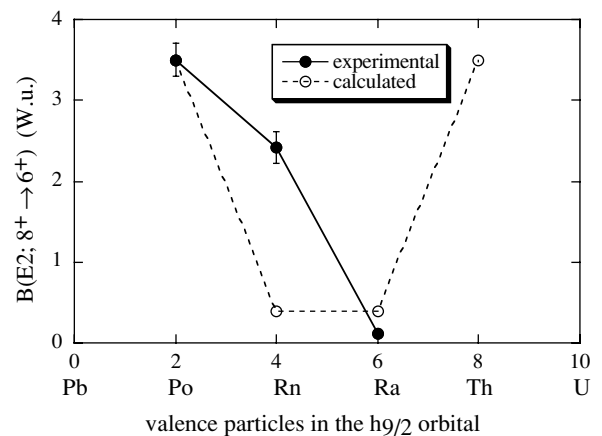


FIG. 4. Calculated (open circles) and experimental [filled circles ([12,15] and this work)]  $B(E2; 8^+ \rightarrow 6^+)$  values for the  $N = 120$  isotones. The calculated transition probabilities are normalized to the experimental values of Po. For  $^{204}\text{Po}$  and  $^{206}\text{Rn}$ , the  $8_1^+ \rightarrow 6_1^+$  transition is used, and for  $^{208}\text{Ra}$ , the  $8_1^+ \rightarrow 6_2^+$  transition is shown. The  $8_1^+ \rightarrow 6_2^+$   $B(E2)$  value of  $^{208}\text{Ra}$  lies closer to zero than does the  $8_1^+ \rightarrow 6_2^+$  value.

$^{206}\text{Rn}$  is significantly higher than would be expected for good seniority ( $<1$  W.u.; see Fig. 4).

Surprisingly, the next higher element,  $^{208}\text{Ra}$ , is in better agreement with the seniority predictions; see Fig. 4. The  $B(E2; 8^+ \rightarrow 6_2^+)$  value is  $0.11(3)$  W.u., while the  $B(E2; 8^+ \rightarrow 6_1^+)$  value is only  $0.0014(3)$  W.u.

Nonetheless, the observation of two  $6^+$  states below the  $8^+$  isomer in  $^{208}\text{Ra}$  suggests that the seniority scheme may not be valid for  $N = 120$ . Two  $6^+$  levels are also known in the  $^{204}\text{Po}$  isotone, although the  $6_2^+$  state lies  $323$  keV above the proposed  $\pi 1h_{9/2}$   $8^+$  isomer. A second  $6^+$  state below the  $8^+$  isomer has been observed in  $^{206}\text{Rn}$ ; however, the isomeric state only decays to the lower  $6^+$  level. A  $g$ -factor measurement of the  $8^+$  isomer in  $^{206}\text{Rn}$  supports a  $\pi 1h_{9/2}$  configuration [16]; it is plausible that the  $6_2^+$  state in this isotope has a large  $\pi 2f_{7/2}^2$  component. For  $N = 120$ , neutrons filling the  $2f_{5/2}$  orbital may cause the  $2f_{7/2}$  proton orbital to be lowered in energy relative to the  $1h_{9/2}$ .

In  $^{208}\text{Ra}$ , isomeric branching to *both*  $6^+$  states is observed. In addition, it is unlikely that the  $8^+$  isomeric level is a relatively pure  $1h_{9/2}^2$  proton configuration. Systematics for this region are plotted in Fig. 5. As the neutron number decreases from  $N = 126$ , and the proton number increases from  $Z = 84$ , the  $\pi 1h_{9/2}$   $8^+$  isomer excitation energy increases. A second  $8^+$  state, suggested as a  $\pi 1h_{9/2}\pi 2f_{7/2}$  two-quasiparticle configuration, remains relatively constant at an excitation energy of  $\sim 2100$  keV. Only one  $8^+$  state has been identified in  $^{208}\text{Ra}$ ; the observed excitation energy ( $2150$  keV) agrees with systematic trends expected for either the  $\pi 1h_{9/2}^2$  or the  $\pi 1h_{9/2}\pi 2f_{7/2}$  configuration.

Below the  $8^+$  isomer, two decay branches, the  $6_2^+ \rightarrow 4_2^+ \rightarrow 2^+$  and the  $6_1^+ \rightarrow 4_1^+ \rightarrow 2^+$ , are observed. The  $6_2^+$  level decays largely to the  $4_2^+$  level;  $[B(M1; 6_2^+ \rightarrow 6_1^+)/B(E2; 6_2^+ \rightarrow 4_2^+)] = 0.00096(22)$ . A transition from the  $6_2^+ \rightarrow 4_1^+$  is not observed, although it would be energetically favored. A similar situation arises in  $^{204}\text{Po}$ ; the yrast  $6^+$  state at  $1627$  keV decays largely to the higher-lying  $4^+$  level  $[B(E2; 6^+ \rightarrow 4_2^+)/B(E2; 6^+ \rightarrow 4_1^+)] \approx 6$ . This would suggest that the lower  $4^+$  state may be of a different character than the decaying  $6^+$  level, similar to that which has been observed in the  $N = 122$  isotones. For the  $N = 122$  nuclei, the yrast  $4^+$  level was attributed to a  $(\nu 2f_{5/2}^2 + \nu 2f_{5/2}3p_{3/2})$  neutron excitation [5]. A similar trend is observed for the  $N = 120$  isotones; the  $4_1^+$  states of  $^{204}\text{Po}$ ,  $^{206}\text{Rn}$ , and  $^{208}\text{Ra}$  are observed at a similar excitation energy as the  $4_1^+$  state of singly magic  $^{202}\text{Pb}$ , as shown in Fig. 5.

The  $B(E2; 6^+ \rightarrow 4_2^+)/B(E2; 6^+ \rightarrow 4_1^+)$  in  $^{210}\text{Ra}$  is equivalent to the ratio in  $^{204}\text{Po}$  ( $\approx 6$ ). If a similar value is expected for  $^{208}\text{Ra}$ , a  $B(E2; 6_2^+ \rightarrow 4_2^+)/B(E2; 6_2^+ \rightarrow 4_1^+) = 6$  suggests that  $\sim 135$  counts would be expected at  $923$  keV in the subtracted spectrum shown in Fig. 1(b) for the  $6_2^+ \rightarrow 4_1^+$  transition. No counts are observed at this energy above background levels, suggesting that the structure of the  $4_1^+$  state in  $^{208}\text{Ra}$  may not be significantly due to the neutron excitation.

The short half-life of the  $^{208}\text{Ra}$  isomer provided an extra challenge for this experiment. The flight time for fusion evaporation recoils from the target position to the solar cell array was approximately  $800$  ns for this reaction. The

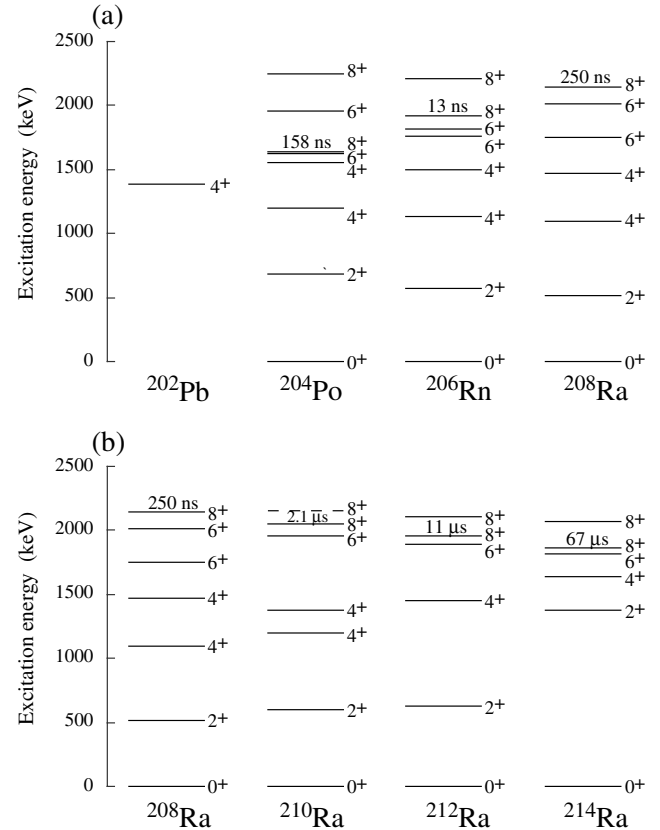


FIG. 5. Systematics of the (a)  $N = 120$  isotones and (b)  $Z = 88$  isotopes. Data are from Refs. [3–5,12,15,17] and this work. The second  $8^+$  state was not observed in  $^{210}\text{Ra}$  [5] but is proposed to lie at the energy shown.

percentage of decays lost in flight is estimated by

$$\frac{\Delta N}{N_0} = \frac{N_0 - N_0 e^{-\frac{\ln(2)}{t_{1/2}} t_{\text{flight}}}}{N_0} = 1 - e^{-\frac{\ln(2)}{t_{1/2}} t_{\text{flight}}}, \quad (1)$$

where  $N_0$  is the number of initial ions,  $t_{1/2}$  is the half-life, and  $t_{\text{flight}}$  is the flight time through the spectrometer. The measured half-life for  $^{208}\text{Ra}$  is  $250$  ns, suggesting that  $89\%$  of the recoils decay prior to implantation at the exit of SASSYER.

An additional challenge was the low cross section for  $^{208}\text{Ra}$  production. Although absolute cross sections were not measured in this experiment, relative cross sections may be roughly estimated. The number of initial ions ( $N_0$ ) is determined by

$$N_0 = \frac{\text{counts}}{e^{-\frac{\ln(2)}{t_{1/2}} t_1} - e^{-\frac{\ln(2)}{t_{1/2}} t_2}}, \quad (2)$$

where  $t_{1/2}$  is the half-life, and  $t_1, t_2$  are the time limits for detecting *counts* decays. In this experiment,  $t_1 = 800$  ns and  $t_2 = 3800$  ns. If it is assumed that  $^{210}\text{Ra}$  is produced *only* from  $^{30}\text{Si}$  interactions with the  $^{184}\text{W}$  atoms in the target and that  $^{208}\text{Ra}$  is produced *only* from  $^{30}\text{Si} + ^{182}\text{W}$ , the relative cross section can be described by

$$\frac{\sigma_{210}}{\sigma_{208}} = \frac{N_0^{210} N_T^{182}}{N_0^{208} N_T^{184}}, \quad (3)$$

where  $N_0^{210}/N_0^{208}$  is the ratio of  $^{210}\text{Ra}$  to  $^{208}\text{Ra}$  initial ions produced in the reactions, and  $N_T^{182}/N_T^{184}$  is the relative abundance of  $^{182}\text{W}$  and  $^{184}\text{W}$  present in the target material. This simple description implies that the  $^{210}\text{Ra}$  production cross section is  $\sim 13$  times larger than  $^{208}\text{Ra}$ . This is not surprising; in the earlier Ra investigation, a factor of 10 difference in cross section was given for the  $^{174}\text{Yb}(^{40}\text{Ar},4n)^{210}\text{Ra}$  relative to the  $^{172}\text{Yb}(^{40}\text{Ar},4n)^{208}\text{Ra}$  reaction [10]. This earlier work reported a  $^{172}\text{Yb}(^{40}\text{Ar},4n)^{208}\text{Ra}$  cross section of  $100 \mu\text{b}$  [10], which is comparable to a result of  $43 \mu\text{b}$  from a study using the  $^{181}\text{Ta}(^{31}\text{P},4n)^{208}\text{Ra}$  reaction [18]. The present study [ $^{182}\text{W}(^{30}\text{Si},4n)^{208}\text{Ra}$ ] is very likely to be within the same range.

## V. CONCLUSIONS

In conclusion, we have measured delayed  $\gamma$ -ray spectra for  $N = 120$   $^{208}\text{Ra}$ . A 250(30)-ns isomer has been observed

and is suggested to be  $J^\pi = 8^+$ . The proposed decay scheme compares favorably with expectations from neighboring Ra isotopes and Po, Rn isotones.

The presence of two  $6^+$  states fed by the  $8^+$  isomer highlights the diminished strength of the proton  $1h_{9/2}$  spherical orbital. In addition, decays from the  $6_2^+$  level differ from the neighboring isotone  $^{204}\text{Po}$  and isotope  $^{210}\text{Ra}$ . Further studies of the Ra isotopes to lower neutron numbers are necessary to fully understand the role of the second  $4^+$  and  $6^+$  states.

## ACKNOWLEDGMENTS

Work supported by U.S. D.O.E. under Grant Nos. DE-FG02-91ER-40609, DE-FG03-03NA-00081, and DE-FG02-94-ER9834, by the National Nuclear Security Administration under the Stewardship Science Academic Alliances program through DOE Research Grant No. DE-FG03-03NA-00081, by Canadian NSERC, and by EPSRC(UK).

- 
- [1] R. Julin, K. Helariutta, and M. Muikku, *J. Phys. G* **27**, R109 (2001).  
 [2] D. J. Dobson *et al.*, *Phys. Rev. C* **66**, 064321 (2002).  
 [3] Y. A. Akovali, *Nucl. Data Sheets* **76**, 127 (1995).  
 [4] T. Kohno, M. Adachi, S. Fukuda, M. Taya, M. Fukuda, H. Taketani, Y. Gono, M. Sugawara, and Y. Ishikawa, *Phys. Rev. C* **33**, R392 (1986).  
 [5] J. J. Ressler *et al.*, *Phys. Rev. C* **69**, 034331 (2004).  
 [6] K. Hauschild *et al.*, *Phys. Rev. Lett.* **87**, 072501 (2001).  
 [7] J. J. Ressler *et al.*, *Phys. Rev. C* **69**, 034317 (2004).  
 [8] J. P. Greene (private communication).  
 [9] J. J. Ressler *et al.*, *Nucl. Instrum. Methods B* **204**, 141 (2003).  
 [10] J. F. C. Cocks and the JUROSPHERE Collaboration, *J. Phys. G* **25**, 839 (1999).  
 [11] D. A. Meyer *et al.* (to be published).  
 [12] E. Browne, *Nucl. Data Sheets* **88**, 29 (1999).  
 [13] R. S. Hager and E. C. Seltzer, *Nucl. Data, Sect. A* **4**, 1 (1968).  
 [14] A. R. Poletti, G. D. Dracoulis, and C. Fahlander, *Phys. Rev. Lett.* **45**, 1475 (1980).  
 [15] M. R. Schmorak, *Nucl. Data Sheets* **72**, 409 (1994).  
 [16] K. H. Mair, D. J. Decman, H. Grawe, H. Haas, and W.-D. Zeits, *Hyperfine Int.* **9**, 87 (1981).  
 [17] M. R. Schmorak, *Nucl. Data Sheets* **80**, 647 (1997).  
 [18] D. D. Bogdanov *et al.*, *Phys. At. Nuclei* **61**, 727 (1998).